

Convergent polynomial expansion, lines of zeros, and slopes of diffraction scattering

M. K. Parida

Physics Department, Sambalpur University, Jyoti Vihar, Burla 768017, Sambalpur, Orissa, India

(Received 16 September 1975; revised manuscript received 8 September 1976)

Using Mandelstam analyticity and conformal mapping new variables are constructed so as to extend the domain of applicability of the convergent polynomial expansion (CPE) to all energies. It is found that the CPE exists for all energies if the scattering amplitude possesses at least one zero in the physical region. The CPE goes over to the optimized polynomial expansion (OPE) for higher energies. The approach from CPE to OPE is faster the higher the energy is, the farther the left-hand cut is than the right-hand cut, and the closer the position of zero is to the backward direction. The variables are found to be potentially useful in describing diffraction scattering at forward angles at all energies. A universal formula has been developed that relates slope parameters to equations of boundaries of spectral functions and lines of zeros. The formula gives a good account of the world data on shrinkage, antishrinkage, and shrinkage-antishrinkage of forward peaks at all energies. Good fits to the data on shrinkage for pp and K^+p scattering, and antishrinkage in $\bar{p}p$ scattering have been obtained with known theoretical boundaries and suitable lines of zeros. Reasonably good fits to the data for K^-p and $\pi^\pm p$ scattering with oscillations at lower energies have been obtained with effective shapes of spectral functions and suitable lines of zeros. In some cases our lines of zero found from this analysis appear to be different from those of Odorico. From the present approach to the scattering problem we observe that the imaginary part of the amplitude that yields $b(s) \rightarrow \infty$ for some values of s must vanish at one point at least in the backward hemisphere.

I. INTRODUCTION

Many models have been proposed to explain hadron-hadron collisions at high energies. Most of the results derived from these high-energy models have also been used to account for the experimental data at lower energies without caring for the range of validity of these results. Recent attempts to explain observed variations of slopes of diffraction scattering fall under this category. A short review of experimental data and theoretical models has been reported in Ref. 1. None of the models developed so far account even qualitatively for the observed experimental data at all energies. Although shrinkage of forward peaks for pp and K^+p scattering has been explained, there does not exist even a qualitative explanation of the shrinkage-antishrinkage pattern observed in $\bar{p}p$, K^-p , π^+p , and π^-p scattering. Experimental data² on slopes of $\bar{p}p$ scattering show rapid decrease with energy at lower and intermediate energies approaching a constant value at higher energies. In this case the slope parameter appears to go to infinity as threshold is approached. Although the data at lower energies for K^-p scattering are too erratic, the slope parameter oscillates at lower energies falling off to a constant value at higher energies. In π^+p scattering a majority of data points at lower energies show antishrinkage. At intermediate energies the slope parameter oscillates and at higher energies it increases with energy. There are clear evidences of rapid decrease at lower energies, oscillations at intermediate

energies, and increase at higher energies in the case of experimental data on slopes of π^-p scattering.

Very good fits to the oscillatory pattern in the case of K^-p , π^+p , and π^-p scattering have been proposed by Barger and Cline³ in a model with an empirical merger of the Regge and geometrical pictures. But their work has been strongly criticized by Weare,⁴ who has pointed out that the energy range in which the model should work is much larger than the authors³ have used in their calculation. It has also been shown that there is not even a qualitative explanation of the shrinkage-antishrinkage at lower and intermediate energies. The empirical extrapolation rule proposed by Barger, Geer, and Phillips⁵ fails to account for the world data on shrinkage-antishrinkage at lower and intermediate energies.

Recently Leader and Pennington^{6,7} have proposed a new kinematic variable, n^2 , for the description of scattering at high energies. Scattering amplitudes are considered as functions of s and n^2 , and asymptotic formulas for $s \rightarrow \infty$ are derived. These formulas have been used to fit the data on the slope parameter at all energies starting from threshold values.⁶ This theory gives a very good description of shrinkage of forward peaks for pp and K^+p scattering, whereas antishrinkage in $\bar{p}p$ scattering predicted by this theory⁷ is much slower in comparison with the experimental data. While the theory is designed for asymptotic energies, data at lower energies have been used⁶ to demonstrate its success. Therefore a similar criticism to that of

Weare⁶ stands against it.

The conventional partial-wave expansion for the spinless-particle scattering amplitude converges within the Lehmann ellipse in the $\cos\theta$ plane. In the limit of very high energies the Lehmann ellipse shrinks onto the physical region making the Legendre expansion unreliable. By means of conformal mapping and the optimized polynomial expansion, the rate of shrinking has been sufficiently slowed down.⁸ As a remedy to such shrinking a parabolic variable was suggested⁹ to describe high-energy scattering of hadrons. At high energies and at forward angles scattering is almost pure imaginary. Experimental data at forward angles can, therefore, serve as a good guide in obtaining information about the imaginary part at nearby unphysical regions. Following up this idea formulas were derived¹ which could successfully correlate experimental data on slopes of forward peaks with equations to boundaries of spectral functions. From fits to the data on slope parameters for pp and K^+p scattering effective shapes of spectral functions were computed. But the same type of approach resulted in the shrinkage of forward peaks of $\bar{p}p$ and K^-p scattering also. Further the formulas are found to yield shrinkage in the cases of π^+p and π^-p scattering. We suppose that the failure of the formulas proposed in Ref. 1 to describe antishrinkage of forward peaks at lower and intermediate energies may be connected with the length of the physical region appropriate for expansion in terms of Laguerre polynomials. In earlier works the appropriate physical region is achieved only at asymptotic energies, and therefore the same type of criticism as before can be raised against them.

In this work we aim at proposing a phenomenological theory for all energies. We demonstrate that such a theory is possible if one makes use of analyticity properties and information about zeros of scattering amplitude. Many attempts have been made to obtain information about zeros of scattering amplitude at high energies.¹⁰⁻¹² Starting from the assumptions of axiomatic field theory Roy¹¹ and Auberson, Kinoshita, and Martin¹² have shown that a Pomeranchuk-theorem-violating amplitude may have some zeros on the physical region in the complex t plane. Odorico has extracted lines of zeros from experimental data according to which^{13,14} the zeros propagate in a systematic manner even up to lower energies in the Mandelstam plane. In the present work, using Mandelstam analyticity and the assumption of the existence of zeros on the physical region, we propose new variables by means of conformal mapping with a view to provide a global understanding of diffraction scattering at forward angles. Although the

variables introduce certain kinds of spurious branch points in the mapped plane we obtain the following results:

(i) There exists a convergent polynomial expansion (CPE) for the scattering amplitude at all energies if it possesses at least one zero on the physical region.

(ii) The CPE goes over to the optimized polynomial expansion (OPE) at high energies. The approach from CPE to OPE is faster the farther the left-hand cut is than the right-hand cut and the closer the position of zero is to the backward direction.

(iii) Using the CPE a universal formula for slope parameters has been derived that relates the slope parameter to the equations to boundaries of spectral functions and lines of zeros for several processes. Thus the formula serves as a method of determining effective shapes of spectral functions and lines of zeros from experimental data.

(iv) Good fits to the data on pp , $\bar{p}p$, and K^+p scattering at all energies have been obtained with elastic boundaries and suitable lines of zeros. The formula gives reasonably good fits to the data on shrinkage-antishrinkage with oscillations at lower energies for π^+p , π^-p , and K^-p scattering with effective shapes of spectral functions and suitable lines of zeros. Our analysis in some cases favors Odorico¹⁴ lines of zeros, whereas they appear to be different in other cases.

(v) From the present approach to the scattering problem we conclude that the imaginary part of the amplitude that yields $b(s) \rightarrow \infty$ must vanish at one point at least, in the backward hemisphere.

In Sec. II we construct new parabolic variables in terms of which convergent polynomial expansion is possible for all energies. The importance of such variables in describing forward (backward) scattering has been pointed out and a universal formula for slope parameters has been derived in this section. In Sec. III the formula is applied to forward diffraction scattering and effective shapes of spectral functions and lines of zeros have been derived. In Sec. IV we discuss our results and indicate further application of this type of analysis.

II. THE CONFORMAL MAPPING AND CONVERGENT POLYNOMIAL EXPANSION

In this section we construct new conformally mapped variables which extend the domain of applicability of CPE to all energies. It is argued that a Laguerre-polynomial expansion in terms of these variables with appropriate weight factor should describe scattering at all energies. In the present work we do not include resonances ex-

licitly, neither do we make any attempt to fit the oscillatory pattern of the data on slope parameters, but we assume that our formula serves as a good shape factor for all energies. We observe that simple considerations of Mandelstam analyticity and zeros of scattering amplitude can account for a good average of the data near the forward directions at all energies. We will follow the notations of Ref. 1.

To develop a new variable for hadron-hadron collisions at all energies we make two important observations upon earlier works.^{1,9}

The first observation is that in Ref. 1 the x plane was folded in such a way that the start of the left- and right-hand cuts coincided. The physical assumption involved in coinciding the start of the cuts was to weight equally the right- and the left-hand-cut contributions. The cuts in the x plane were mapped onto the branches of a parabola in the z plane with origin as focus. The forward direction ($x=1$) was mapped into origin and the left- and the right-hand cuts were symmetrically placed with respect to the physical region in the z plane. Because of the fact that the left- and the right-hand cuts are symmetrically placed with respect to the physical region in the z plane contributions due to both the cuts were weighted equally. Further, the unknown parameters in the series for OPE, being fixed by the experimental data in the physical region, the differential cross section will be the same at equivalent points on both the cuts. Although such a feature is desirable in the processes like pp scattering, it is not desirable for processes exhibiting asymmetric cut plane of analyticity. For energies above threshold the right-hand cut is closest to the forward direction, whereas the left-hand cut is farther away in the x plane. Even for processes with symmetric cut plane of analyticity, forces represented by the right-hand cut have more influence over scattering in the forward hemisphere. The right-hand cut is considered so important that Lovelace¹⁵ has ignored the presence of the left-hand cut as compared to it in his analysis of the diffraction scattering data by conformal-mapping methods. We devise a mapping which places the start of the right-hand cut closest to the origin and the start of the left-hand cut infinitely far removed from it in the z plane. Such a mapping function gives nonzero values of slope parameter near threshold. But it fails to account for the shrinkage-antishrinkage pattern.

The second observation is that the physical region $-1 \leq x \leq +1$ is mapped onto a segment of the real axis in the z plane, which in the limit $s \rightarrow \infty$ spreads the entire right half of the real axis from zero to infinity. It is well known that,^{9,16} when the domain of analyticity is a parabola with origin as

focus, a series in Laguerre polynomials converges in the interior of the parabola. The physical region for Laguerre-polynomial expansion is the semi-infinite line from $z=0$ to $z=\infty$. In the conformal maps^{1,9} the physical region spreads the right half of the real axis in the z plane like $(\ln s)^2$ as $s \rightarrow \infty$. Thus only in the asymptotic energy region the representation

$$\frac{d\sigma}{dt} \equiv f(s, z) = e^{-\alpha z} \sum_n a_n(s) L_n(2\alpha z) \quad (1)$$

is accurately valid. We think that this might be a possible region for disagreement with the lower and intermediate energy data for $\bar{p}p$, π^+p , π^-p , and K^-p scattering. To find a convergent representation for all energies we construct a new conformally mapped parabolic variable that gives the correct physical region for Laguerre-polynomial expansion at all energies.

According to our first observation the conformal mapping that places the start of the right-hand cut closest to and the start of the left-hand cut infinitely far removed from the image of the forward direction can be written in terms of a parabolic variable

$$z_0(s, x) = (\cosh^{-1} \sqrt{\omega_0})^2 \quad (2a)$$

with

$$\omega_0(s, x) = \left(\frac{x_- + 1}{x_+ - 1} \right) \left(\frac{x_+ - x}{x_- + x} \right). \quad (2b)$$

This conformal transformation maps the right-hand cut in the x plane [Fig. 1(a)] onto a crescent that forms the forward portion of the parabola, the start of the right-hand cut lying at the apex, and the left-hand cut onto the branches of the parabola in the z_0 plane [Fig. 1(b)]. The forward direction ($x=1$) is mapped onto the origin which is the focus of the parabola in the z_0 plane. Since the right-hand cut is squeezed onto the forward portion that covers the origin uniformly and the left-hand cut is mapped onto the remaining parts of the branches of the parabola which lie farther away from the origin, we suppose this type of mapping to take into account of the relative weight between the left- and the right-hand cut. Now using z_0 instead of z and taking only the first term in the expansion (1) then gives¹ the slope parameter in the forward direction as

$$b(s) = \frac{\alpha}{t_R} \left(1 + \frac{t_R}{4q^2 + t_L - \Delta/s} \right). \quad (3)$$

When compared with the corresponding formula of Ref. 1 we note a sign change before the second term in the bracket in formula (3). Apparently this means that if the formula of Ref. 1 accounted for shrinkage, formula (3) may account for anti-shrinkage. Calculated values of slope parameter

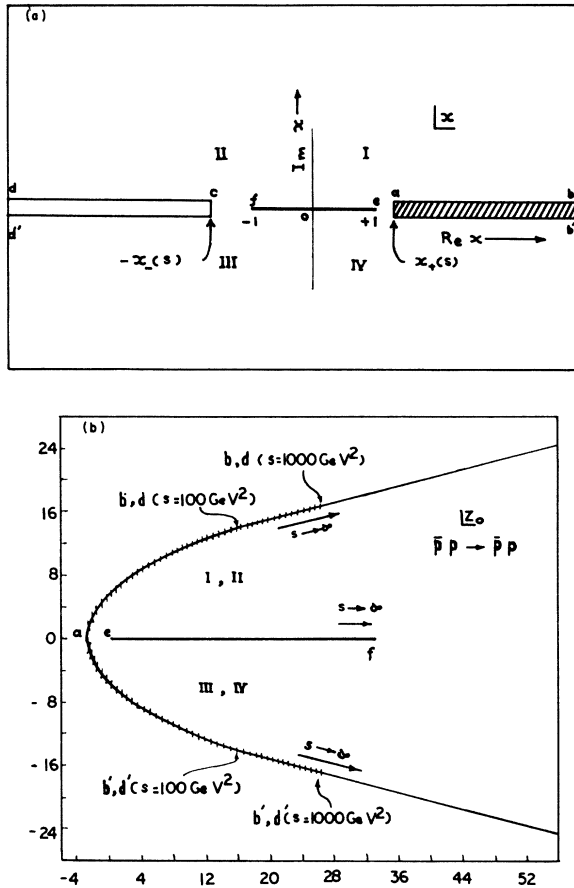


FIG. 1. (a) Complex $x = \cos\theta$ plane illustrating analytic properties of the imaginary part of two-body scattering amplitude. (b) Conformal transformation into z_0 plane defined by Eq. (2).

for $\bar{p}p$ scattering have been shown in Fig. 4. It is found that although formula (3) gives a nonzero value of slope parameter at threshold there is not even a qualitative explanation of the antishrinkage pattern. Such a situation arises because of the smallness of $4q^2$ compared to t_L near threshold and the additional s dependence in $t_R(s)$. We suppose that the failure of such a mapping function to explain low-energy data may be due to finite length of the physical region in the z plane at finite energies.

Before proceeding further we observe that the conformal mapping of formula (2) does not introduce spurious cuts. In Ref. 1 a square transformation has been used which introduces spurious cuts by folding a part of the physical region on top of the other part. However, formula (3) is not quantitatively satisfactory.

We now construct another variable that contains the good feature according to our first observation and conforms to the appropriate physical region at

all energies as pointed out in our second observation. This is possible if the amplitude possesses at least one zero on the physical region. Such a variable is obtained most simply by multiplying the variables proposed earlier^{1,9} and in Eq. (2) by a function $g_n(x)$, real and positive everywhere on the real axis, and possessing n poles on the physical region at x_1, x_2, \dots, x_n in the x plane. Thus our new variable is

$$z_n(s, x) = g_n(x) z \quad (4)$$

with

$$g_n(x) = (1+x)^{2n} \prod_{i=1}^n (x-x_i)^2, \quad (5)$$

where z represents variables proposed earlier^{1,9} and in Eq. (2). The real and imaginary parts of z_n , when x lies on the cuts in the x plane satisfy the relation

$$(\text{Im } z_n)^2 = \pi^2 g_n(x) [\text{Re } z_n + \frac{1}{4} \pi^2 g_n(x)]. \quad (6)$$

One can use the factor $(c+x)^{2n}$ instead of $(1+x)^{2n}$ in $g_n(x)$, where c is any real constant. We have chosen $c=1$ for the sake of simplicity and to avoid another free parameter. This choice, of course, introduces strong behavior at the point $x=-1$, which is not far away in the z_n plane. Considered as a function of x , $g_n(x)$ appears to possess a zero of order $2n$ at $x=-1$, and n poles each of order 2 in the x plane. But when looked as a transformation of the cut x plane, the many-sheet structure is folded together introducing spurious cuts in the $g_n(x)$ plane or equivalently in the z_n plane. Since the mapping of Eq. (4) introduces branch points which may influence convergence of polynomial expansion, it is important to realize their locations in the mapped plane. For a general $g_n(x)$ as given by Eq. (5) location of such branch points may be complicated. But we will see in the subsequent sections that $z_1(x)$ gives a global understanding about slopes of diffraction scattering. Therefore, we have studied locations of branch points for simple cases. Let us consider the case of a particular $z_n(x)$ for which $x_1=x_2=\dots=x_n$. In this case there are two spurious branch points each of order $2n$ in the z_n plane at $z_n=0$ and $z_n=\infty$. Similarly there are two branch points at exactly the same locations in the z_1 plane but each of order 2. Thus in both these cases, one of which is relevant for data analysis, the spurious cut completely overlaps the physical region appropriate for Laguerre-polynomial expansion in the mapped plane. Ciulli⁸ has discussed convergence of polynomial expansion in terms of a mapped variable which introduces an "artificial" cut explicitly along the physical region. Although the spurious cut has been finally removed on physical grounds⁸ the conver-

gence phenomena have been shown to hold true even in the presence of such cuts. We, therefore, suppose that the spurious cuts will cause no problem for convergence in the simple cases as long as they lie on the physical region or outside the figure of convergence.

The mapping function (4) does not map the cuts onto a regular figure of convergence. However, for the distant parts of the cuts satisfying $|x| \gg 1 \gg |x_t|$, $g_n(x) = 1$, and hence the real and the imaginary parts of z_n satisfy the equations of a parabola. The physical region in the x plane is mapped onto the right half of the real axis in the z_n plane for all energies. Such a possibility has been achieved due to the presence of poles of the function $g_n(x)$. When z_n is used in place of z we observe that the representation (1) yields zeros of the scattering amplitude at the n points corresponding to the poles of $g_n(x)$ on the physical region. We assume that these zeros are in general energy dependent. We further note that the existence of only one zero on the physical region is sufficient to guarantee the physical region appropriate for Laguerre polynomial expansion at all energies. Probably this is the requirement if one wishes to obtain a physical region of infinite length in the z plane from that of finite length in the x plane. By the function z_n , however, the cuts do not map onto any regular figure of convergence at all energies. It has been proved by Cutkosky and Deo⁸ and Ciulli⁸ that the greater the convergence of the polynomial expansion is, the larger the area of the cut plane of analyticity mapped onto the interior of the figure of convergence is. The convergence is maximum when the entire cut plane of analyticity is mapped onto the interior, the cuts forming the boundary of the figure of convergence. By the conformal mapping (4) the branch points do always remain away from the physical region in the z_n plane. Thus there exists a parabolic figure of convergence, its boundary touching the image of some point(s) on the cuts, with correct physical region for Laguerre-polynomial expansion in the z_n plane. Then the Laguerre-polynomial expansion in terms of z_n is convergent at all energies. But since this figure of convergence contains only a part of the image of the entire cut plane of analyticity the convergence is not maximum. We shall presently show that for a simple $g_n(x)$, the domain of convergence is greater the higher the energy is, the farther the left-hand cut is than the right-hand cut, and the closer the position of zero is to the backward direction. In fact it is possible to achieve maximum convergence at high energies. The same type of reasoning also may hold for the convergence of Laguerre-polynomial expansion in terms of $z_n(x)$. Even though the convergence of expansion in terms

of z_n is not maximum at finite energies, only the first few terms in the expansion will contribute to scattering in the forward direction since $z_0 \approx -t/t_R$, for $4q^2 + t_L \gg |t|$ and $|t| \ll t_R$.

For simplicity let us consider the case when the forward amplitude has only one zero in the backward hemisphere with $x_1 = -x_0(s)$. The mapping function becomes

$$z_1 = (1+x)^2 z_0(s, x) / (x+x_0)^2. \quad (7)$$

It is found that, although the image of the right-hand cut deviates only slightly at lower energies,¹⁷ the image of the left-hand cut does not lie on any regular figure of convergence in the z_1 plane. At fixed s the deviation of the image of the left-hand cut from the parabola is less the closer the position of zero is to the backward direction and the farther the left-hand cut is than the right-hand cut in the x plane. In plotting the conformal transformation we have used¹⁴

$$x_0(s) = 1 - 0.7/2q^2 \quad (8)$$

for pp and $\bar{p}p$ scattering and

$$x_0(s) = 1 - 0.15/2q^2 \quad (9)$$

for pp scattering corresponding to crossover zeros.¹⁸ The conformal transformations have been shown in Figs. 2(a), 2(b), and 2(c) for pp and $\bar{p}p$ scattering illustrating our conclusions. The conformal transformations for π^+p , π^-p , K^+p , and K^-p scattering behave in the same fashion as that for $\bar{p}p$ scattering. It is found in general that a domain of convergence exists for all energies for all scattering processes in the z_1 plane. This domain of convergence is larger the more the asymmetry of the cut plane of analyticity is and the closer the position of zero is to backward direction. As energy increases the domain of convergence increases and at high energies the images of the left- and right-hand cuts approach lying on a parabola corresponding to the figure of convergence of Laguerre polynomial expansion. Thus the convergent polynomial expansion becomes maximally convergent⁸ at high energies.¹⁹

As we have already discussed the conformal transformation has been constructed to describe scattering data at forward angles where the right-hand cut has more influence. Similarly a conformal transformation can be constructed so as to account for scattering in the backward hemisphere where the left-hand cut has more influence. In the special case with only one zero in the forward hemisphere at $x = x_1(s)$, the transformation can be written as

$$z_0(s, x) = (1-x)^2 z_{0b}(s, x) / [x - x_f(s)]^2, \quad (10)$$

where

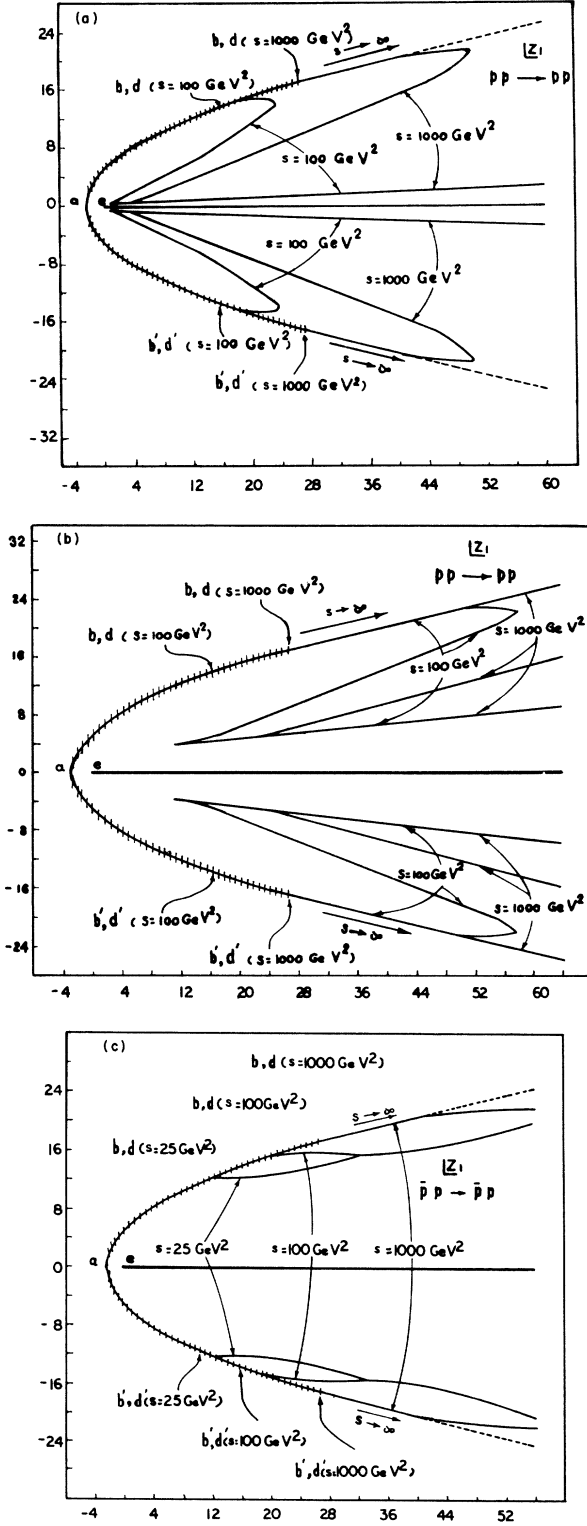


FIG. 2. Conformal transformation into z_1 plane with (a) $x_0(s) = 1 - 0.7/2 q^2$, (b) $x_0(s) = 1 - 0.15/2 q^2$ for different energies for pp scattering, and (c) $x_0(s) = 1 - 0.7/2 q^2$ for different energies for $\bar{p}p$ scattering.

$$z_{0b}(x) = (\cosh^{-1} \sqrt{\omega_{0b}})^2 \quad (11a)$$

with

$$\omega_{0b} = (x_- + x)(x_+ + 1) / [(x_+ - x)(x_- - 1)]. \quad (11b)$$

For an asymmetric cut plane of analyticity the amplitude can be parametrized as

$$f(s, x) = e^{-\alpha z_1} \sum_n b_n L_n(2\alpha z_1) + e^{-\beta z_b} \sum_n c_n L_n(2\beta z_b). \quad (12)$$

It may be noted that for processes like pp scattering possessing $t \leftrightarrow u$ symmetry, $x_+ = x_-$, and the symmetry can be explicitly preserved by taking $|x_0(s)| = |x_f(s)|$, a pair of symmetrically placed zeros and putting $\beta = \alpha$, $b_n = c_n$, for $n = 0, 1, 2, \dots$. This reduces the number of parameters in (12) by one half. We note that near backward angles and high energies

$$z_1 \simeq \frac{u^2}{(u - u_0)^2} (\ln s)^2. \quad (13)$$

Thus the contribution of the forward amplitude is damped out with energy in the backward direction. A further damping is provided by the closeness of u_0 to $u = 0$. Similarly the backward amplitude given in terms of z_b is damped out in the forward direction. Thus for scattering near forward directions we can write from (12), by retaining terms first order in t , to a good approximation as

$$f(s, x) \simeq b_0 e^{-\alpha z_1} + c_0. \quad (14)$$

Similarly the first term in the second series in (12) contributes to angular distribution near backward directions. We will use formula (14) to obtain a universal formula for the slopes of diffraction scattering and parametrize the experimental data for different diffractive processes. As has been discussed earlier the variables z_1 and z_b introduce spurious cuts on the physical region in the mapped planes.

III. UNIVERSAL FORMULA FOR SLOPE PARAMETERS, LINES OF ZEROS, AND EFFECTIVE SHAPES OF SPECTRAL FUNCTIONS

In this section we use our CPE to derive a universal formula for slopes of forward peaks in terms of lines of zeros and shapes of spectral functions. It has been demonstrated that such a formula describes very well the world data on shrinkage, antishrinkage, and shrinkage-antishrinkage of forward peaks at all energies. While analyzing the data for various processes we are not disheartened if we get a χ^2/N_{DF} (N_{DF} = number of degrees of freedom) larger than what is expected

of a good fit, because, as we have emphasized in the beginning of Sec. II, no attempt is made here to include resonances explicitly or to fit the oscillatory patterns with a large number of parameters. Even then our fits are found to be better in view of the discussion made in the Introduction. Lines of zeros and effective shapes of spectral functions have also been computed from the experimental data. We define the slope parameter of the forward peak as

$$b(s) = \frac{d}{dt} \ln \left(\frac{d\sigma}{dt} \right) \Big|_{t=0} \quad (15)$$

and use formulas (2), (6), (7), (8), and (12) to obtain expressions for $b(s)$ for two-body elastic scattering of unequal masses as²⁰

$$b(s) = \frac{16\alpha q^4}{[4q^2 + u_0(s) - \Delta/s]} \frac{1}{t_R} \times \left(1 + \frac{t_R}{4q^2 + t_L - \Delta/s} \right). \quad (16)$$

A similar expression²⁰ for the slope of backward scattering can also be derived. In Eq. (16) $u_0(s)$ corresponds to the position of the zero in the backward hemisphere whose s dependence can be obtained from the equation to the line of zero in the Mandelstam plane. Here t_R and t_L can be obtained from equations to the boundaries of spectral functions as discussed in Ref. 1. We note that $u_0(\infty) = \text{const.}$ thus $\lim_{s \rightarrow \infty} b(s) = \text{const.}$ It is also possible for certain values of s and shapes of lines of zeros $[4q^2 + u_0(s) - \Delta/s] = 0$, in which case $b(s) = \infty$. Thus we conclude that the imaginary part of the forward scattering amplitude, that yields large values of slope parameter for some value of s , must possess at least one zero in the backward hemisphere. We will presently see that such a behavior of the slope parameter is consistent with the experimental data for $\bar{p}p$ scattering. We next proceed to analyze the experimental data for various diffractive processes² by means of formula (16). If the process under consideration is $a + b \rightarrow a + b$ we will replace α , Δ , t_R , and t_L by α_{ab} , Δ_{ab} , t_{Rab} , and t_{Lab} , respectively. Our approach is as follows: We first use known equations for lines of zeros and boundaries of spectral functions and examine the agreement of formula (16) with experimental data. Whenever there is disagreement we use new parametrizations for lines of zeros and shapes of spectral functions until there is agreement and thus compute effective shapes of spectral function and lines of zeros. We find that the formula (16) is universal in the sense that it describes very well the experimental data on slopes of pp , $\bar{p}p$, K^+p , and π^+p scattering.

A. pp scattering

Odorico^{13,14} has extracted lines of zeros for pp scattering and many other processes from experimental data. It has been suggested that a Krisch type²¹ of variable describes the lines of zeros in the Mandelstam plane:

$$\frac{u_0(s) t_0(s)}{s} = a, \quad (17)$$

where $u_0(s)$ and $t_0(s)$ are u, t values lying on a line of zero. One of the values of a has been found to be¹⁴ -0.7 GeV^2 . A slightly different type of line of zeros has been suggested by Pinsky.²² From (17) we have

$$u_0(s) = \frac{-4q^2 \pm (16q^4 - 4as)^{1/2}}{2}. \quad (18)$$

Choosing the positive sign before the radical we obtain with the help of (16) and (18)

$$b_{pp}(s) = \frac{16\alpha_{pp} q^4}{[2q^2 + (4q^4 - as)^{1/2}]^2} \frac{1}{t_{Rpp}} \times \left(1 + \frac{t_{Rpp}}{4q^2 + t_{Lpp}} \right), \quad (19)$$

where the theoretical elastic boundaries of spectral functions are given by¹

$$t_{Rpp} = t_{Lpp} = 4m_\pi^2 + \frac{4m_\pi^4}{s - 4m^2}. \quad (20)$$

From the expression (19) we observe that the slope parameter and hence the amplitude near forward angles possesses spurious square-root branch points in the s plane at

$$s = s_\pm = 4m^2 \pm 2(4m^2a + a^2)^{1/2}.$$

Such an undesirable feature is the characteristic of the Krisch type of lines of zeros. With the expression (20) and the value of $a = -0.7 \text{ GeV}^2$ determined from the data on differential cross sections, formula (19) has only one free parameter, α_{pp} . The fit to the data^{2,23} at all available energies has been shown in Fig. 3. We find that the fit at high energies is the same as in Ref. 1, giving good account of the shrinkage of diffraction peak. The formula of Ref. 1 yielded negative values of slope parameter near threshold; the present formula yields $b_{pp}(s) \propto q^4$ for s near threshold. It may be noted that, whereas effective shapes of spectral functions were necessary to fit the data with three free parameters, the present analysis gives a reasonably good fit with elastic boundary and one parameter only:

$$\alpha_{pp} = 0.877. \quad (21)$$

The value of χ^2/N_{DF} for the fit is 14.9. Most of the

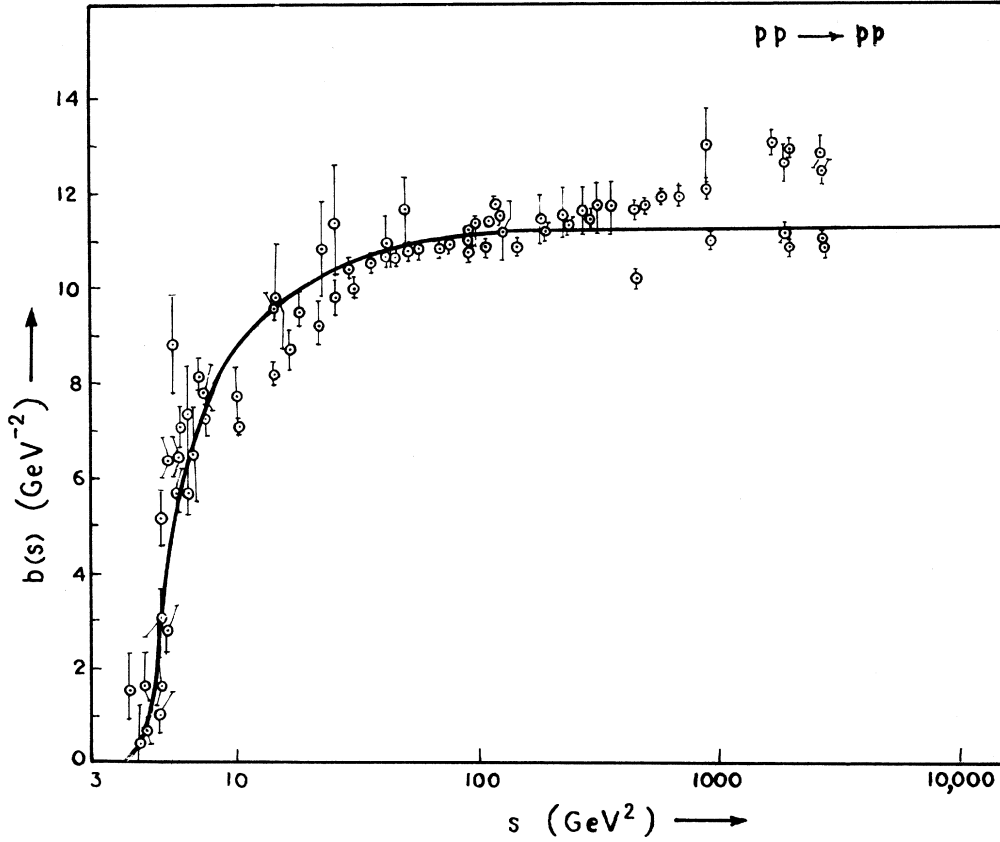


FIG. 3. Slope parameter of the forward peaks for pp scattering as a function of s . The solid curve is the result of this analysis. The data points are from Refs. 2 and 23.

contributions to the χ^2 value come from very-high-energy data points for which our formula yields constant slope. Presumably the fit at ultrahigh energies may be improved if one exploits s -plane analyticity also. In this analysis and subsequent analyses we do not suppose it is meaningful to evaluate uncertainties of parameters because of the larger χ^2 value.

B. $\bar{p}p$ scattering

Experimental data on $\bar{p}p$ scattering show rapid antishrinkage of the forward peak at lower energies and the slope parameter appears to rise to infinity near threshold. We find that it is impossible to account for this type of behavior with lines of zeros obtained by Odorico^{13,14} and Pinsky,²¹ which give shrinkage of the forward peak like pp scattering. But if we assume existence of a fixed- u line of zeros

$$u_0(s) = c_1, \quad (22)$$

the formula for slope parameter can be written in the following form:

$$b_{\bar{p}p}(s) = \frac{16\alpha_{\bar{p}p} q^4}{(4q^2 + c_1)^2} \frac{1}{t_{R\bar{p}p}} \left(1 + \frac{t_{R\bar{p}p}}{4q^2 + t_{L\bar{p}p}} \right). \quad (23)$$

With elastic boundaries of spectral functions

$$t_{R\bar{p}p} = 4m_\pi^2 + \frac{4m_\pi^4}{s - 4m_\pi^2} \quad (24a)$$

and

$$t_{L\bar{p}p} = 4m^2 + \frac{4m_\pi^4}{s - 4m_\pi^2} \quad (24b)$$

we tried to fit the experimental data by the formula (23), taking $\alpha_{\bar{p}p}$ and c_1 as two unknown parameters. The fit is shown in Fig. 4 (curve II) with

$$\begin{aligned} \alpha_{\bar{p}p} &= 0.974, \\ c_1 &= -0.295 \text{ GeV}^2. \end{aligned} \quad (25)$$

We observe that the slope parameter approaches infinity more sharply near threshold than the experimental data. The rise to infinity can be made slower by choosing a curved line of zeros

$$(s - s_1)[u_0(s) - u_1] = c_2 \quad (26)$$

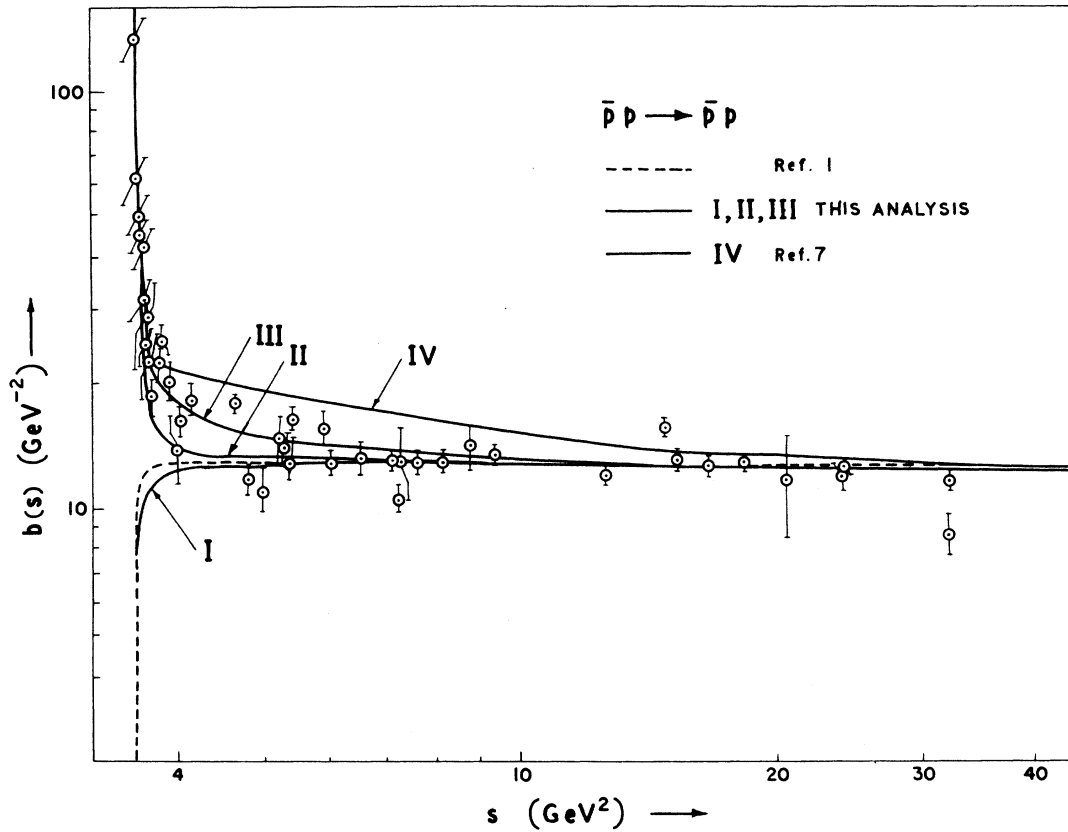


FIG. 4. Slope parameter of the forward peaks for $\bar{p}p$ scattering as a function of s . Curve I is the fit by formula (3). Curve II is the fit by formula (23) with fixed- u line of zeros. Curve III is the fit by formula (27) with curved line of zeros. Curve IV is the fit as described in Ref. 7. The dotted curve is the fit given in Ref. 1.

such that the formula for slope parameter becomes

$$b_{\bar{p}p}(s) = \frac{16\alpha_{\bar{p}p}q^4}{[4q^2 + u_1 + c_2/(s - s_1)]^2} \frac{1}{t_{R\bar{p}p}} \times \left(1 + \frac{t_{R\bar{p}p}}{4q^2 + t_{L\bar{p}p}} \right). \quad (27)$$

Now choosing $s_1 = u_1$, for the sake of simplicity, formula (27) has three unknown parameters. A very good fit to the data has been obtained for

$$\alpha_{\bar{p}p} = 0.900, \\ s_1 = u_1 = -0.687 \text{ GeV}^2,$$

and

$$c_2 = 2.795 \text{ GeV}^4. \quad (28)$$

The fit is shown in Fig. 4 (curve III). For this fit $\chi^2/N_{DF} = 7.7$. We find²⁴ that the total χ^2 for the fit given by formula (27) is almost half of that for the fit given by formula (23). We have already noted that the Odorico¹⁴ or Pinsky²² type of zero completely fails to account for $\bar{p}p$ data. Our analysis

reveals a new type of lines of zeros. It may be noted that one of the asymptotes to the curve (26), $s_1 = -0.687 \text{ GeV}^2$, is almost the same as that of pp scattering ($a = -0.7 \text{ GeV}^2$). Present data on differential cross sections for $\bar{p}p$ scattering²⁵ indicate existence of dips in the backward hemisphere. Further high-energy experiments for $\bar{p}p$ backward scattering in the range $-1 \text{ GeV}^2 < u < 0$ will decide whether such new lines of zeros are present. For comparison we have also shown the fit by the formula of Leader and Pennington⁷ in Fig. 4 (curve IV). The dotted curve in Fig. 4 represents the fit as proposed in Ref. 1 for elastic ρ_{ut} and effective ρ_{su} . We find that our formula gives the best account of the experimental data at all energies in comparison to all the existing theories.

C. K^+p scattering

The boundaries of ρ_{st} , being nearer to the forward direction for energies above threshold, its structure plays an important role on scattering.

Approximate hyperbolic shapes of ρ_{st} and ρ_{su} were assumed and effective shapes of spectral functions were computed from fits to the experimental data in Ref. 1. Here we theoretically deduce²⁶ equa-

$$t_1 = 4m_\pi^2 + 4m_\pi^2 [4m^2 m_X^2 + m_\pi^2 m_X^2 - 2m_\pi m_X (m^2 + m_X^2) + 2sm_\pi m_X] / [s - (m + m_X)^2] [s - (m - m_X)^2] \quad (29a)$$

for $s > (m + m_X)^2$, where $m_X = m_\pi + m_K$, and

$$t_2 = 16m_\pi^2 + 32m_\pi^2 m_K^2 m^2 \frac{\left\{ 2m_\pi^2 \left(\frac{1}{m^2} + \frac{1}{m_K^2} \right) - \frac{m_\pi^2}{mm_K} - \frac{m^2 + m_K^2 - s}{2mm_K} \left[2m_\pi \left(\frac{1}{m_K} - \frac{1}{m} \right) + \frac{2m_\pi^2}{m^2} + \frac{2m_\pi^2}{mm_K} + 1 \right] \right\}}{[s - (m + m_K)^2] [s - (m - m_K)^2]} \quad (29b)$$

for $s > (m + m_K)^2$. Thus t_{RK^+p} is given by the minimum of t_1 and t_2 given by Eqs. (29a) and (29b).

Theoretical deductions of equations to the boundaries of ρ_{su} appear to be tedious. Therefore, we assume an approximate shape¹

$$t_{LK^+p} = (m + m_K)^2 + \frac{4m_\pi^4}{s - (m_\Delta + m_\pi)^2}. \quad (30)$$

The formula for slope parameters for K^+p scattering can be written as

$$b_{K^+p}(s) = \frac{16\alpha_{K^+p} q^4}{[4q^2 + u_0(s) - \Delta_{K^+p}/s]^2} \frac{1}{t_{RK^+p}} \times \left(1 + \frac{t_{RK^+p}}{4q^2 + t_{LK^+p} - \Delta_{K^+p}/s} \right). \quad (31)$$

Reasonably good fit to the experimental data^{2,27} by this formula and with a fixed u line of zero has

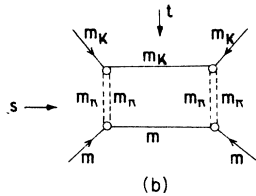
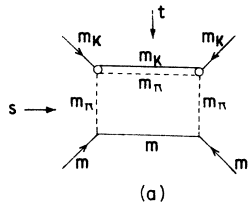


FIG. 5. Box diagram for KN scattering with (a) two-pion exchange, and (b) four-pion exchange, in the t channel.

tions to the boundaries of spectral functions by taking box diagrams shown in Figs. 5(a) and 5(b). Thus we get two different equations for two different energy ranges:

been shown in Fig. 6 with

$$\alpha_{K^+p} = 0.575, \quad (32)$$

$$u_0(s) = 1.5 \text{ GeV}^2.$$

We observe that the line of zeros lies in the unphysical region. For this fit $\chi^2/N_{DF} = 15.9$.

D. K^-p scattering

For KN scattering equations to the boundaries of ρ_{ut} are derived from those of ρ_{st} by replacing s by u . Thus for K^-p scattering $t_{RK^-p} = t_{RK^+p}$, and $\Delta_{K^-p} = \Delta_{K^+p}$, if we ignore mass difference between K^+ and K^- mesons. Thus the formula for slope parameters in this case is the same as Eq. (31) except that the constant α_{K^+p} is replaced by α_{K^-p} . Fit to the data using elastic boundaries and a fixed- u line of zeros with

$$\alpha_{K^-p} = 0.572 \quad (33)$$

$$u_0(s) = 0.088 \text{ GeV}^2$$

has been shown in Fig. 7 (curve II). We observe that curve II gives a good qualitative description of the data at lower and intermediate energies. The fit can be improved if an effective shape is taken for ρ_{ut} . For this purpose we replace the pion mass before the square bracket in the second term in Eq. (29a) and before the large curly bracket in the second term in Eq. (29b) by a variable parameter λ . Since the left-hand cut is farther away we do not suppose that the slope parameter would be sensitive to the changes of the shape of t_{LK^-p} . Thus taking $t_{LK^-p} = t_{LK^+p}$ we obtain a good fit to the data (curve I, Fig. 7) for

$$\alpha_{K^-p} = 0.572, \quad (34)$$

$$\lambda = 0.031 \text{ GeV},$$

and

$$u_0(s) = 0.088 \text{ GeV}^2.$$

For this fit $\chi^2/N_{DF} = 10.8$. We find that our formula

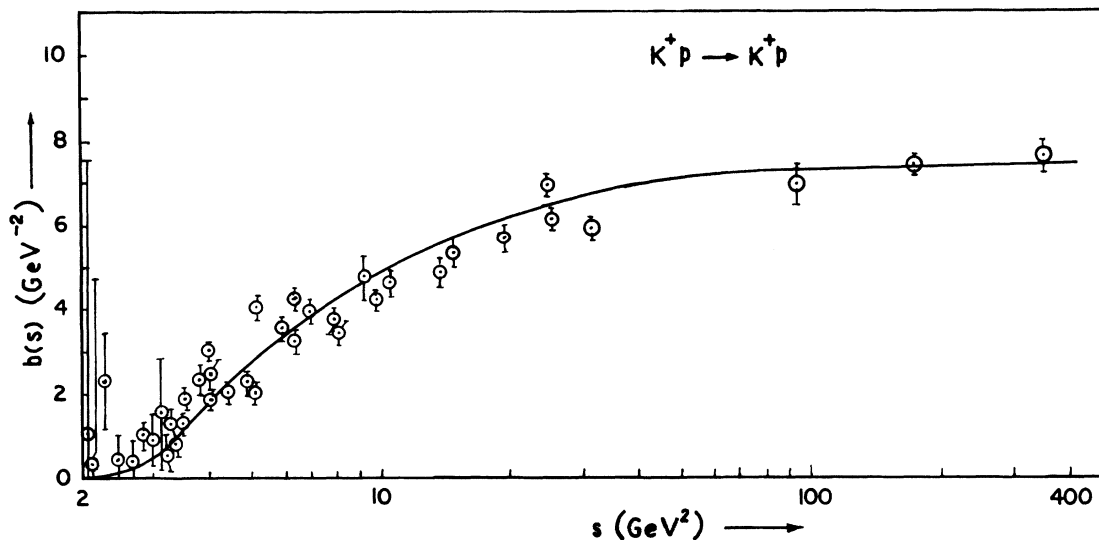


FIG. 6. Slope parameter of the forward peak for K^+p scattering as a function of s . The solid curve is the result of this analysis. Data points are from Refs. 2 and 27.

yields oscillations at lower energies. In the present case the data at lower energies are so erratic that we do not feel the need for using a curved line of zeros for analysis. According to Odorico¹⁴ the lines of zeros at high energies are all fixed- u lines with a $\sim 1 \text{ GeV}^2$ spacing which is a characteristic of the Veneziano formula. Our line of zeros $u_0(s)$

$= 0.088 \text{ GeV}^2$ does not coincide with the analysis of Odorico.¹⁴ The disagreement may be due to following reasons: First, our analysis is based on inaccurate data. Second, Odorico has extracted lines of zeros of nondiffractive parts of the amplitudes whereas we are concerned with the diffractive part.

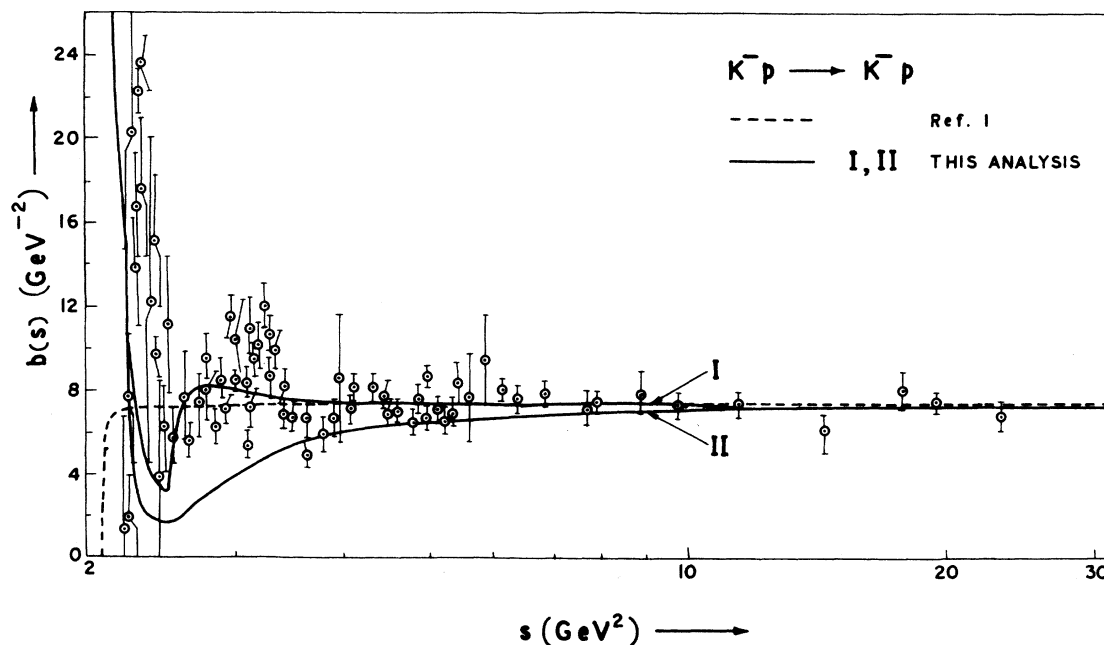


FIG. 7. Slope parameter of the forward peaks for K^-p scattering as a function of s . Curve I is the fit with effective boundary and fixed u line of zeros. Curve II is the same fit with elastic boundary. The dotted curve is the fit given in Ref. 1. The data points are from Ref. 2.

E. π^+p scattering

It is well known that²⁴ $t_{R\pi^+p}$ is the minimum of

$$t_1 = 16m_\pi^2 + \frac{64s\lambda^4}{[s - (m + m_\pi)^2][s - (m - m_\pi)^2]} \quad (35a)$$

for $s > (m + m_\pi)^2$, and

$$t_2 = 4m_\pi^2 + \frac{16\lambda^4(s + 3m^2 - 3m_\pi^2)}{[s - (m + 2m_\pi)^2][s - (m - 2m_\pi)^2]} \quad (35b)$$

$$t_1 = m^2 + m_\pi^2 + 8m_\pi^2(m^2s - \Delta_{\pi N}) / \{[s - (m + 2m_\pi)^2][s - (m - 2m_\pi)^2]\} \\ + \left\{ 4m^2m_\pi^2 + \frac{64m_\pi^4(m^2s - \Delta_{\pi N})^2}{\{[s - (m + 2m_\pi)^2][s - (m - 2m_\pi)^2]\}^2} + \frac{4m^2s(m^2 + m_\pi^2) + 3m^2\Delta_{\pi N} + 2m_\pi^2\Delta_{\pi N} + 4s\Delta_{\pi N}}{[s - (m + 2m_\pi)^2][s - (m - 2m_\pi)^2]} \right\}^{1/2} \quad (36a)$$

for $s > (m + 2m_\pi)^2$,

$$t_2 = m^2 + 4m_\pi^2 + 8m_\pi^2(m^2s - \Delta_{\pi N}) / \{[s - (m + m_\pi)^2][s - (m - m_\pi)^2]\} \\ + \left\{ 16m^2m_\pi^2 + \frac{64m_\pi^4\{(m^2s - \Delta_{\pi N})^2 + 16[4m^2m_\pi^2s(m^2 + 4m_\pi^2) - (2m_\pi^4 + 4m_\pi^2s)\Delta_{\pi N}]\}}{\{[s - (m + m_\pi)^2][s - (m - m_\pi)^2]\}^2} \right\} \quad (36b)$$

for $s > (m + m_\pi)^2$. We tried to parametrize the data on slope parameters for π^+p scattering by the formula (16) with fixed u lines of zeros. Curve I in Fig. 8 represents our fit with

$$\alpha_{\pi^+p} = 0.723, \\ \lambda = 0.253 \text{ GeV}, \\ u_0(s) = 0.288 \text{ GeV}^2. \quad (37)$$

Although our fit describes a good average of the data, the slope parameter rises to infinity at $s = 1.5 \text{ GeV}^2$ corresponding to the zero of $4q^2 + u_0(s) - \Delta_{\pi N}/s$. At lower energy the line of zero passes near the backward direction in the physical region. Experimental data of Bowler *et al.*²⁸ at lower energies indicate strong evidence of dips near the backward angles. The value of χ^2/N_{DF} for this fit is as large as 54.1. Such a large value of χ^2 is due to the oscillatory nature of the slope parameter and the larger population of data points with relatively small errors near the Δ (~ 1900) resonances.² Curve III in Fig. 8 gives the same fit with elastic boundaries $\lambda = m_\pi$.

We also tried to parametrize the data with a curved line of zeros given by Eq. (26). Assuming for the sake of simplicity $u_1 = s_1$, the formula for slope parameters is

$$b_{\pi^+p} = \frac{16\alpha_{\pi^+p}q^4}{[s - \Sigma + u_1 + c_2/(s - u_1)]^2} \frac{1}{t_{R\pi^+p}} \\ \times \left(1 + \frac{t_{R\pi^+p}}{4q^2 + t_{L\pi^+p} - \Delta_{\pi N}/s} \right). \quad (38)$$

for $s > (m + 2m_\pi)^2$, which represent theoretical boundaries of ρ_{st} for $\lambda = m_\pi$. Since the left-hand cut in the x plane is farther away than the right-hand cut from the forward direction we suppose that the slope parameter for π^+p scattering may not be sensitive to the changes of shapes of ρ_{su} . Therefore we have chosen the elastic boundary of ρ_{su} given by the minimum of t_1 and t_2 :

where $\Sigma = 2(m^2 + m_\pi^2)$. Fit to the data by this formula has been shown in Fig. 8 (curve II) with

$$\alpha_{\pi^+p} = 0.519, \\ \lambda = 0.178 \text{ GeV}, \\ c_2 = 1.031 \text{ GeV}^4, \quad (39)$$

and

$$u_1 = -0.195 \text{ GeV}^2.$$

The χ^2/N_{DF} value for this fit is 25.7, which is almost half of that for the fit (37). In spite of the smaller value of χ^2 it is clear that visually curve II is a worse fit than curve I. This is because curve II has fitted the average of the data near Δ (~ 1900) resonances in a better fashion. Although this fit accounts for the data only qualitatively one of the asymptotes to the line of zero is very close to that obtained by Odorico¹⁴ ($u = -0.2 \text{ GeV}^2$). We will presently see that a curved line of zero gives a good account of the π^-p data.

F. π^-p scattering

Equations to the boundaries of ρ_{ut} for πN scattering are derived from those of ρ_{st} by replacing s by u . Thus $t_{R\pi^-p}$ and $t_{L\pi^-p}$ are taken to be the same as those for π^+p scattering. Fit to the data taking fixed u lines of zero and effective shapes of spectral functions with

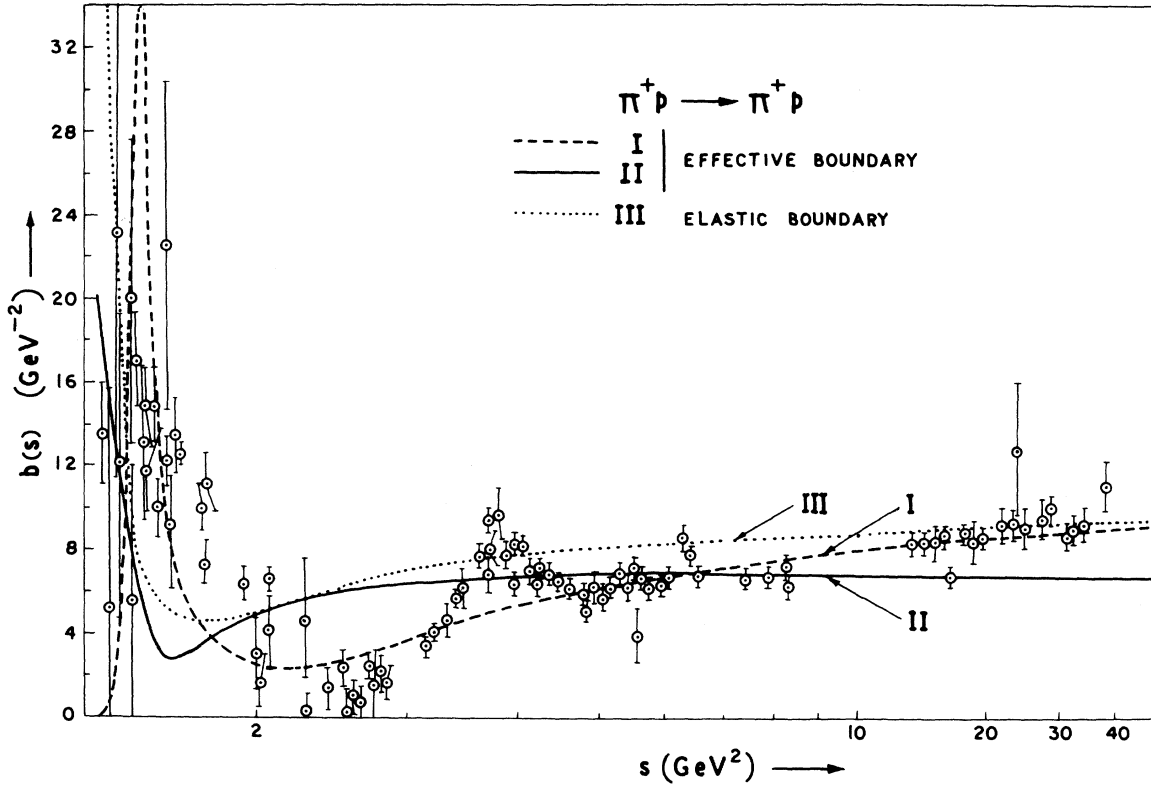


FIG. 8. Slope parameters for the forward peaks for $\pi^+ p$ scattering as a function of s . Curve I is the fit with effective boundary and fixed u line of zero. Curve III is the fit with elastic boundary and fixed u line of zeros. Curve II is the fit with effective boundary and curved line of zeros. The data points are from Ref. 2.

$$\begin{aligned}\alpha_{\pi-p} &= 0.75, \\ \lambda &= 0.187 \text{ GeV},\end{aligned}$$

and

$$u_0(s) = 0.302 \text{ GeV}^2,$$

is shown by curve I in Fig. 9. Although the fit describes a good average of the data, the slope parameter rises to infinity at $s \approx 1.5 \text{ GeV}^2$ as in the case of $\pi^+ p$ scattering. Curve III in Fig. 9 is the fit with elastic boundaries, $\lambda = m_\pi$. Next we tried to fit the data with a curved line of zero as given by formula (38). Good average of the data on shrinkage-antishrinkage with oscillations at lower energies is described by the fit with

$$\begin{aligned}\alpha_{\pi-p} &= 0.664, \\ \lambda &= 0.200 \text{ GeV}, \\ c_2 &= 0.98 \text{ GeV}^4,\end{aligned}\tag{44}$$

and

$$u_1 = -0.195 \text{ GeV}^2.$$

This fit has been shown by curve II in Fig. 9. The

χ^2/N_{DF} for this fit is 14.7. We find that the infinity has been removed and very near the threshold the slope parameter rises to a value in agreement with the data. The slope parameter also falls to zero at threshold in this fit. Such a fit has been possible because of the closeness of the zero of $s - \Sigma + u_1 + c_2/(s - u_1)$ to threshold where the numerator damps out the large values. We note that¹⁴ one of the asymptotes to the curved line of zeros is close to $u_0(s) = -0.2 \text{ GeV}^2$. In the next section we discuss our results of data analysis obtained in this section.

IV. RESULTS AND DISCUSSION

It is well known that the usual partial-wave expansion for scattering amplitudes converges within the Lehmann ellipse. This ellipse shrinks onto the physical region like $\sim 1/s$ as $s \rightarrow \infty$. In the optimized polynomial expansion for scattering amplitude, developed by Ciulli, Cutkosky, and Deo⁸ shrinking has slowed down. The ellipse in this case shrinks like $\sim 1/(\ln s)^4$. As a remedy to such shrinking parabolic mapping was suggested^{1,9} for high-energy scattering of hadrons. In such type of

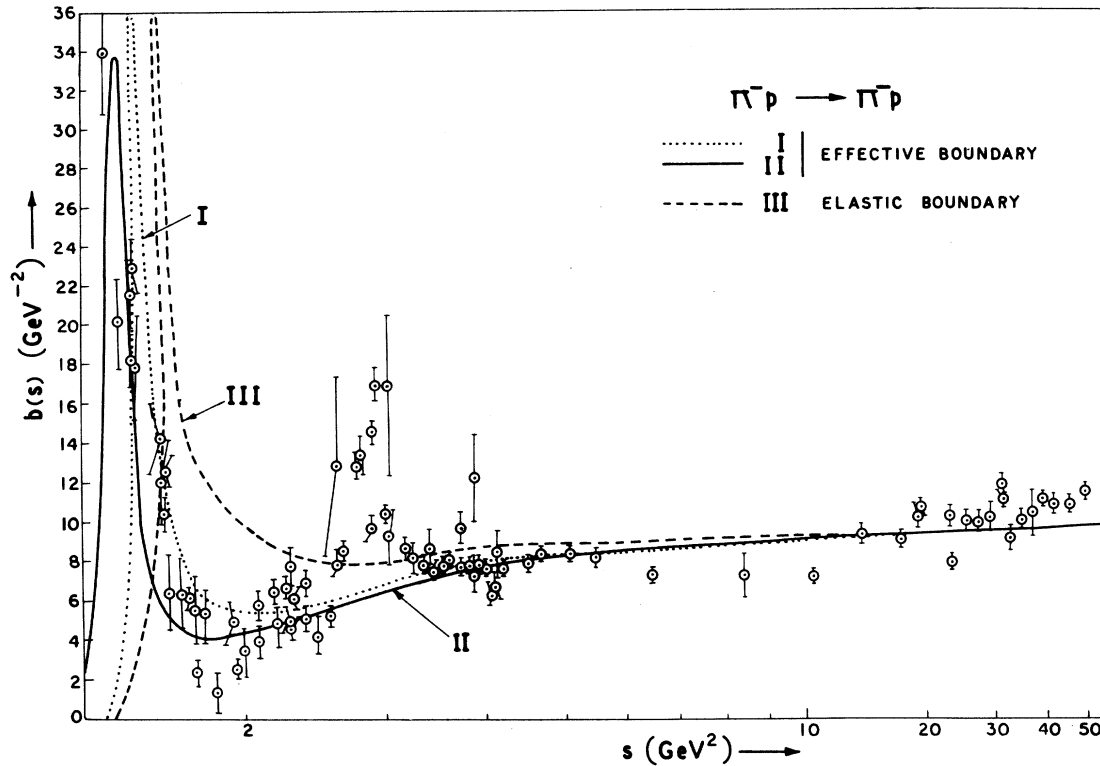


FIG. 9. Slope parameter of the forward peaks for $\pi^- p$ scattering as a function of s . Curve I is the fit with effective boundary and fixed u line of zeros. Curve II is the fit with effective boundary and curved line of zeros. Curve III is the fit with elastic boundary and fixed u line of zeros. The data points are from Ref. 2.

mapping the boundary remained fixed but the physical region moved like $\sim(\ln s)^2$ in the z plane as $s \rightarrow \infty$. Thus the physical region appropriate for Laguerre-polynomial expansion was achieved only at asymptotic energies. It was found¹ that only shrinkage of forward peaks could be explained by this variable. In Ref. 1 a square transformation has been used which introduces spurious branch points in the mapped variable plane by folding a part of the physical region on top of the other part. In the present work we have at first proposed a new variable z_0 which does not introduce spurious branch points in the mapped plane. But we find that such a variable is not quantitatively satisfactory to explain antishrinkage. In this case also the physical region is mapped onto only a part of the right half of the real axis at finite energies. Next we have proposed new variables which map the physical region onto the right half of the real axis in the mapped plane at all energies. In the mapped plane the image of the physical region remains fixed for all energies whereas the image of the cuts change their shapes with energy, but they always remain away from the image of the physical region. But again such transformations

introduce spurious branch cuts which overlap the image of the physical region in the mapped plane. For such simple variables, one of which has been used for data analysis, there is no problem for convergence of Laguerre-polynomial expansion.⁸ From physical grounds Ciulli⁸ has discussed how to remove such cuts. At present we do not find any means of removing such cuts from the mapped plane. Subject to this limitation our conclusion is that it is possible to have a CPE for all energies if the amplitude possesses at least one zero on the physical region in the x plane. A particular case is considered when the amplitude possesses only one zero in the backward hemisphere. In such type of "parabolic" mapping the right-hand cut is mapped onto the forward portion of the parabola with focus at the origin in the z_1 plane even at moderate energies.¹⁷ However, the left-hand cut is mapped onto a curve which approaches the remaining portion of the parabola at high energies. Thus CPE is possible at high energies and at high energies the CPE goes over to OPE. The approach from CPE to OPE is faster, the farther the left-hand cut is than the right-hand cut and the closer the position of zero is to the backward direction.

If one ignores the singularities due to the left-hand cut it is possible to have OPE in terms of z_1 even at moderate energies.¹⁷

It is believed that scattering at high and low energies is connected by analyticity properties. We have been able to develop CPE for all energies using analyticity properties. Previous works^{1,3,6,7,9} are subject to criticism when they are used to fit the data at all energies because of their validity in the asymptotic energy range only. But our CPE has been developed to be valid at all energies and, therefore, is free of such criticism.⁴

Besides the limitation due to the presence of spurious cuts one of the main objections which may be raised against this CPE is that it is not optimized at lower and intermediate energies. We have some comments regarding this point. Firstly, the convergence of this series is better (may be much better) than the convergence of the series in Legendre polynomials in $\cos\theta$ even at lower energies. The domain of convergence in the latter case is the Lehmann ellipse which forms a very small part of the entire cut plane of analyticity. In the present case the domain of convergence contains a much larger part of the image of the cut plane of analyticity by mapping. Secondly, criticisms²⁹ have been raised against accelerated convergence of OPE and new types of conformal mapping have been proposed³⁰ where emphasis upon a regular figure of convergence has been relaxed. Thirdly, even if the convergence may be poor in the worst possible case, it does not affect our analysis of data near forward directions as the variables are proportional to $|t|$ in this region. The proposed CPE in terms of new parabolic variable is bound to be potentially useful in describing forward scattering data except for the limitation due to spurious cuts. As it has been pointed out in Sec. II we could have chosen $(c+x)^{2n}$ instead of $(1+x)^{2n}$ in the numerator of $g_n(x)$, where c is any real constant. For the present analysis we have taken $c=1$ to avoid another free parameter. This choice would give rise to a peak of the forward amplitude in the backward direction. Similarly the backward amplitude expanded in terms of z_n gives a peak in the forward direction. These peaks, of course, have zero slopes. Strong behaviors of this kind can be avoided by replacing unity by suitable real constants which may be determined by data analysis.

We have also proposed how to parametrize the data at backward angles using this type of approach. It has been shown how to preserve $t \rightarrow u$ symmetry explicitly in the case of pp scattering. We have derived a universal formula for slope parameter that relates the slope parameter to equations of boundaries of spectral functions and lines of zeros.

For the first time we have given a formula which accounts for the world data on shrinkage, anti-shrinkage, and shrinkage-antishrinkage at all energies when effective shapes of spectral functions and lines of zeros are taken judiciously. Thus we have developed a method of obtaining effective shapes of spectral functions and lines of zeros using analyticity properties and experimental data on slope parameters. From the present approach to the scattering problem we conclude that the imaginary part of the amplitude, that yields $b(s) \rightarrow \infty$ for some values of s , must have at least one zero in the backward hemisphere.

Our formula provides a good fit to the data on slopes of pp scattering with a constant value of slope at high energies with elastic boundaries and the Odorico^{13,14} line of zero. We find that it is not possible to explain the data for $\bar{p}p$ scattering at all energies with the Odorico or Pinsky²² type of zeros. On the other hand we find a good fit to the data at all energies accounting for large values of slope near threshold with a fixed u line of zero. A still better fit is obtained with a curved line of zeros, one of whose asymptotes is the line $u = -0.687 \text{ GeV}^2$. The presence of such zeros can be verified by backward $\bar{p}p$ scattering experiments at high energies. The presence of dips in the backward hemisphere is indicated in the experimental data²⁶ on differential cross sections. A good account of shrinkage in K^+p scattering^{2,31} has been obtained with elastic boundaries of spectral functions and a fixed u line of zero. Reasonably good fits to the data with shrinkage, antishrinkage, and oscillations at lower energies have been obtained for K^-p and π^+p scattering. Introducing curved lines of zeros eliminates infinities in slope parameters for π^+p scattering, but visually worsens the fit for π^+p scattering although it improves the fit for π^-p scattering. However, one of the asymptotes to such curved line of zero is very close to the line of zero due to Odorico.¹⁴

We find that a line of zeros of the Krisch type introduces spurious branch points in the s plane. On the other hand fixed u or other types of curved u lines of zeros taken for various fits introduce poles in $b(s)$ and hence zeros in the near forward amplitude in the s plane. One of the reasons for relatively larger values of χ^2/N_{DF} obtained by our fits for π^+p and K^-p scattering is due to the fact that the effect of resonances has not been included explicitly in our formula. For scattering of spinless particles the Veneziano model predicts the zero trajectories to be straight lines with $u = \text{const}$ passing through the intersections of a pair of resonances. That the lines of zeros are straight lines described in the real Mandelstam plane can be derived on the assumption¹⁴ that the amplitude has

the same residues at each of the two resonances which have zero widths. But in practice the residues are not equal and the resonances have finite widths, thus the zero trajectories are neither real nor linear and they have imaginary parts. A method of analysis of two-body reactions by conformal mapping and by using zero trajectories has been proposed by Barrelet,³¹ who has pointed out that the trajectories are complex and curved. We feel that the imaginary parts of the zero trajectories may be used to eliminate infinities which appear at unwanted values of s for π^+p scattering.

To summarize our results on effective shapes of spectral functions we find that elastic boundaries computed from box diagrams could account for the slopes of pp , $\bar{p}p$, and K^+p scattering at all energies. The values of λ computed for the effective shapes ρ_{st} and ρ_{ut} in the case of πN scattering are found to be larger, and that of ρ_{ut} in the case of KN scattering is found to be smaller than the one given by the box diagrams. In the data analysis presented here theoretical boundaries of ρ_{su} for πN and an assumed form of ρ_{su} for KN scattering have been taken for the fits with the assumption that they do not contribute to scattering in the region far away from them. Thus their effective shapes could not be determined by the present analyses. We suggest that the experimental data on the backward slopes for $\pi^+p(\pi^-p)$ and $K^+p(K^-p)$ scattering be used to compute effective shapes of ρ_{su} using the formula for slope parameters as suggested.²⁰ Similarly the forward scattering data on $\pi^+\pi^- \rightarrow \bar{p}p$, and $K^+K^- \rightarrow \bar{p}p$ may be used to obtain information about ρ_{tu} for πN and KN scattering.

We notice that our formula gives constant slope parameter at very high energies. In particular the data for pp scattering²³ show a $\sim \ln s$ type of increase consistent with the exchange of a nearly flat Pomeron. The absence of such energy dependence in our formula may be due to the fact that we have not taken into account the analyticity properties in the s plane. Scattering amplitude is a function of two independent variables and analyticity properties in the planes of both the vari-

ables should be exploited. But while using analyticity properties in the s plane one should also be cautious about the introduction of spurious branch points by the Krisch type of lines of zeros.

One of the most interesting applications of the CPE proposed here would be to search for zeros of scattering amplitudes from differential-cross-section data at various energies and obtain the energy dependence of their positions. As we have pointed out earlier, Odorico¹⁴ has extracted lines of zeros for the nondiffractive part of amplitudes. This technique as described here can be further developed to parametrize differential cross sections with dips in the diffraction region. But before using our representations it is better to remove strong behaviors at points not far away in the z_1 and z_b planes and the spurious branch points.

Our analysis and conclusions in this paper are based upon CPE by conformal mapping and experimental data. But the experimental data are not enough to justify the correctness of the representations and many other representations, different from those used here, are possible. Still then our analysis reveals how simple considerations of Mandelstam analyticity and the hypothesis of the existence of zeros of scattering amplitude may yield a global understanding of diffraction scattering.

ACKNOWLEDGMENT

The author expresses his gratitude to Professor T. Pradhan, Director, Institute of Physics, Bhubaneswar for providing facilities at the Institute where a part of this work was done. He expresses his gratitude to Professor B. M. Udgankar for valuable comments and to Professor V. Singh for many interesting discussions. He wishes to thank Professor S. P. Misra, Dr. S. N. Pattanayak, and Dr. B. Panda for useful discussions. The computational facility of the Computer Centre, Utkal University, is thankfully acknowledged.

¹B. B. Deo and M. K. Parida, Phys. Rev. D **8**, 249 (1973).

²T. Lassinski, R. Levi Setti, B. Schwarzschild, and P. Ukleja, Nucl. Phys. **B37**, 1 (1972).

³V. Barger and D. Cline, Nucl. Phys. **B23**, 227 (1970).

⁴T. J. Weare, Nuovo Cimento **9A**, 173 (1972).

⁵V. Barger, K. Geer, and R. J. N. Phillips, Phys. Lett. **36B**, 35 (1971); **36B**, 350 (1971).

⁶E. Leader and M. R. Pennington, Phys. Rev. Lett. **27**, 1325 (1971).

⁷E. Leader and M. R. Pennington, Phys. Rev. D **7**, 2668 (1973). See especially Eq. (3.10) of this paper for anti-shrinkage of $\bar{p}p$ scattering.

⁸R. E. Cutkosky and B. B. Deo, Phys. Rev. **174**, 1859 (1968); S. Ciulli, Nuovo Cimento **61A**, 787 (1969).

⁹B. B. Deo and M. K. Parida, Phys. Rev. Lett. **26**, 1609 (1971). Here it has been assumed that the differential cross section has the same analytic structure, in the $\cos\theta$ plane, as the scattering amplitude. We will use the terms differential cross section and scattering

amplitude interchangeably for the sake of convenience. By amplitude we mean its imaginary part unless specified otherwise.

- ¹⁰J. Finkelstein, Phys. Rev. Lett. 24, 172 (1970); R. C. Cassela, *ibid.* 24, 1463 (1970); J. D. Bessis, Nuovo Cimento 45A, 974 (1966); and see also Ref. 31.
- ¹¹S. M. Roy, Phys. Lett. 34B, 407 (1971).
- ¹²G. Auberson, T. Kinoshita, and A. Martin, Phys. Rev. D 3, 3185 (1971).
- ¹³R. Odorico, Lett. Nuovo Cimento 2, 835 (1969). In our representation other zeros lying in the physical region may come from the zeros of the series. But here we discuss those zeros inherent in the conformal mapping which are necessary to achieve the correct physical region.
- ¹⁴R. Odorico, Nucl. Phys. B37, 509 (1972); CERN Report No. TH.1271, 1970 (unpublished).
- ¹⁵C. Lovelace, Nuovo Cimento 25, 730 (1962).
- ¹⁶*Higher Transcendental Functions* (Bateman Manuscript Project) edited by A. Erdélyi (McGraw-Hill, New York, 1953), Vol. II, see especially Chap. X.
- ¹⁷The maximum deviation of the image of the right-hand cut from the parabola occurs for the starting point of the cut at which

$$g(x_+) = \left[\frac{1+x}{x+x_0(s)} \right]^2 \Big|_{x=x_+(s)} \\ = \frac{[2+t_R(s)/2q^2]^2}{[2+t_R(s)/2q^2 - \Delta/2q^2 s + u_0(s)/2q^2]^2}.$$

The condition that this expression is close to unity can be expressed for equal-mass scattering as

$$4q^2 + t_R(s) \gg |u_0(s)|. \quad (i)$$

Thus the image of the right-hand cut lies on the parabola, for high energies and zeros closer to the backward direction. The energies at which this inequality is satisfied are termed as "moderate" in this paper. Note that this condition can be satisfied earlier in the energy scale for zeros close to the backward direction. For illustration we have calculated the function $g(x_+)$ for different positions of zero at $s=100 \text{ GeV}^2$, with $t_R=4m_\pi^2$ as

$$g(x_+) = \begin{cases} 1.003, & x_0(s) = 1 - 0.15/2q^2 \\ 0.014, & x_0(s) = 1 - 0.7/2q^2 \end{cases}.$$

For higher energies $g(x_+)$ is still closer to unity.

- ¹⁸G. Brandenburg *et al.*, Phys. Lett. 58B, 367 (1975); R. K. Carnegie *et al.*, *ibid.* 58B, 361 (1975).
- ¹⁹The maximum deviation of the image of the left-hand cut occurs at a point close to the start of the cut. Thus at a point $x = -x_- - \delta$, with δ small and positive,

$$g(-x_- - \delta) = \frac{[(t_L - \Delta/s)2q^2 + \delta]^2}{[(t_L - u_0(s))/2q^2 + \delta]^2}$$

The condition that this expression is close to unity can be written for the equal-mass case as

$$t_L + 2q^2\delta \gg |u_0(s)|. \quad (ii)$$

Thus the inequality becomes stronger the farther the left-hand cut is, the closer u_0 is to the backward direction, and the higher the energy is. For a given t_L , t_R , and u_0 inequality (ii) is satisfied at larger energies than those at which (i), mentioned in Ref. 17, is satisfied. Inequalities (i) and (ii) corroborate our conclusions.

²⁰Owing to the presence of the constant c_0 in Eq. (14) the constant α in Eq. (16) is multiplied by a factor $b_0/(b_0 + c_0)$, which we have omitted for simplicity. The formula for the slope of backward peak, defined as

$$B(s) = \frac{d}{du} \ln \left(\frac{d\sigma}{du} \right) \Big|_{u=0},$$

is found to be

$$B(s) = \frac{16\beta q^4}{[4q^2 + t_1(s)]^2} \frac{1}{(t_L - \Delta/s)} \left[1 + \frac{(t_L - \Delta/s)}{4q^2 + t_R} \right],$$

where

$$x_1(s) = 1 + t_1(s)/2q^2$$

is the position of the zero in the forward hemisphere. We observe that for pp scattering $B(s) = b(s)$.

- ²¹A. D. Krisch, Phys. Rev. Lett. 19, 1149 (1967); in *Boulder Summer School Lectures in Theoretical Physics*, edited by W. E. Brittin and A. O. Barut (Gordon and Breach, New York, 1967), Vol. IX.
- ²²S. S. Pinsky, Phys. Rev. Lett. 27, 1548 (1971).
- ²³V. Bartenev *et al.*, Phys. Rev. Lett. 31, 1367 (1973); G. Barbiellini *et al.*, Phys. Lett. 39B, 663 (1972); U. Amaldi *et al.*, *ibid.* 44B, 116 (1973); G. Beznogikh *et al.*, *ibid.* 43B, 85 (1973).
- ²⁴The total χ^2 for curve II for $\bar{p}p$ scattering is 775 with 49 degrees of freedom, but it is only 365 with 48 degrees of freedom for curve III.
- ²⁵D. Cline *et al.*, Phys. Rev. Lett. 21, 1268 (1968); C. Daum *et al.*, Nucl. Phys. B6, 617 (1968); J. K. Yoh *et al.*, Phys. Rev. Lett. 23, 506 (1969); see also Ref. 22.
- ²⁶J. Hamilton, lectures given at the Neils Bohr Institute and NORDITA, Copenhagen, 1968 (unpublished).
- ²⁷C. W. Akerlof *et al.*, Phys. Rev. Lett. 35, 1406 (1975); 35, 1195 (1975).
- ²⁸M. G. Bowler, R. J. Cashmore, and A. Kaddoura, Nucl. Phys. B37, 133 (1972).
- ²⁹M. L. Griss and G. C. Fox, Phys. Rev. D 7, 74 (1973); the authors have shown that the accelerated-convergence method of phase-shift analysis generates larger high partial waves than the previous analyses. R. A. Arndt, R. H. Hackman, and L. D. Roper, Phys. Rev. Lett. 32, 31 (1974).
- ³⁰A. R. Choudhary, Nuovo Cimento 24A, 161 (1974); Lett. Nuovo Cimento 12, 33 (1975); and ICTP Report No. IC/75/140 (unpublished); A. R. Choudhary and R. B. Jones, J. Phys. A5, 981 (1972).
- ³¹E. Barrelet, Nuovo Cimento 8A, 331 (1972).